Phospholipid Component Volumes: Determination and Application to Bilayer Structure Calculations

Roger S. Armen, Olivia D. Uitto, and Scott E. Feller
Department of Chemistry, Whitman College, Walla Walla, Washington 99362 USA

ABSTRACT We present a new method for the determination of bilayer structure based on a combination of computational studies and laboratory experiments. From molecular dynamics simulations, the volumes of submolecular fragments of saturated and unsaturated phosphatidylcholines in the liquid crystalline state have been extracted with a precision not available experimentally. Constancy of component volumes, both among different lipids and as a function of membrane position for a given lipid, have been examined. The component volumes were then incorporated into the liquid crystallographic method described by Wiener and White (1992. *Biophys. J.* 61:434–447, and references therein) for determining the structure of a fluid-phase dioleoylphosphatidylcholine bilayer from x-ray and neutron diffraction experiments.

INTRODUCTION

Fundamental to any description of membrane structure is the volume occupied by the lipid molecules. Experimental techniques are available for the determination of phospholipid molecular volumes, with a precision of a few Å^3 (Nagle and Wilkinson, 1978; White et al., 1987; Wiener and White, 1992a). More recently (Petrache et al., 1997), it was shown that atomic-level computer simulations offer the opportunity to determine the volumes of arbitrarily defined pieces of the lipid molecule (for an example of one possible definition, see Fig. 1). Information on the volume of these lipid fragments has applications in the design of simple packing models for membranes as well as in methods for the interpretation of NMR and x-ray or neutron diffraction experiments. In this paper we determine fragment volumes for saturated and unsaturated phosphatidylcholines and demonstrate an application of these data in the interpretation of diffraction experiments.

The biologically relevant phase of bilayer membranes is the liquid crystalline (L_α) state, characterized by disordered headgroup and alkyl chain conformations. The inherent disorder in these systems precludes the possibility of an atomic-level structural determination, as is routinely obtained for proteins from x-ray diffraction. Multilamellar dispersions, existing as regular arrangements of stacked bilayers, can be studied as model membranes by such experimental techniques as diffraction (x-ray or neutron) or NMR spectroscopy. These experiments primarily give information on atomic location or conformation as a function of position along the bilayer normal (taken as the *z* axis), or in the case of NMR along the fatty acid chains. Information on the structure in the lateral direction (i.e., the plane of the bilayer) is generally determined through a combination of experimental data and model interpretation. For example, the surface area per molecule, *A*, can be calculated by dividing the volume per lipid or lipid fragment by its projected length along the *z* axis, where this length comes from an interpretation of experimental data. Nagle (1993) has derived a formula for *A* based on the average NMR order parameters (S_{CD}) measured for methylene groups at the top of the fatty acid chains,

$$A = \frac{2 \times V_{CH2}}{(\frac{1}{2} + |\langle S_{CD}^{plateau} \rangle|) \times 1.27} \quad (1)$$

where V_{CH2} is the volume per methylene group. Others (Seelig and Seelig, 1974; Koenig et al., 1997) have used a similar formula, which takes into account the average order parameter of the entire chain,

$$A = \frac{V_{HC}}{(\frac{1}{2} + |\langle S_{CD} \rangle|) \times n \times 1.27} \quad (2)$$

where V_{HC} is the volume of hydrocarbon chains of length *n*. Both of these treatments require knowledge of the volume of each methylene group (Eq. 2 also requires the volume per methyl group). These volumes have traditionally come from comparisons of experimentally determined volumes for lipids (and alkanes) as a function of chain length. The values do not follow unambiguously from experiment, however, because of different treatments of the data. Nagle and Wilkinson (1978) obtained 27.6 and 55.2 Å^3 for methylene and methyl volumes, respectively, by comparing volumes at the same temperature. Small (1986) compared volumes using a reduced temperature (relative to the melting point) and obtained 29.6 and 35.6 Å^3. Because the areas calculated via Eqs. 1 and 2 are directly proportional to the chain segment volumes, any inaccuracies in the volumes will lead

Received for publication 20 January 1998 and in final form 23 April 1998.

Address reprint requests to Dr. Scott Feller, Department of Chemistry, Wabash College, P.O. Box 352, Crawfordsville, IN 47933-0352. Tel.: (765) 361-4535; Fax: (765) 361-6340; E-mail: fellers@wabash.edu.

Mr. Armen's present address is Department of Biomolecular Structure and Design, University of Washington, Seattle, WA.

Ms. Uitto's present address is Department of Chemistry, University of Utah, Salt Lake City, UT 84112-0850.

0006-3495/98/08/734/11 $2.00

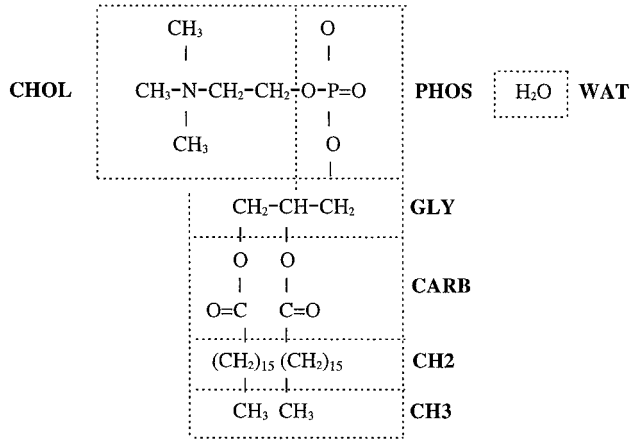

FIGURE 1 Parsing scheme used to describe DPPC. A similar grouping was done for DOPC and POPC, where a new group was added that was composed of the CH=CH segment of the oleic acid chains.

to errors in the estimation of A, a crucial parameter of membrane structure.

The interpretation of diffraction experiments on fluid phase bilayers also requires the volumes of lipid fragments. Nagle et al. (1996) describe several methods for estimating A from diffraction data that require the volume per methylene, volume per methyl, and the volume per headgroup. In addition to the aforementioned difficulties in determining hydrocarbon volumes, the volume per headgroup must come from results on gel phase lipid bilayers. Apart from the issue of average component volume of lipid, a second question arises in the analysis of both x-ray and NMR data as to the constancy of methylene and water volume. For example, does the volume per water molecule near the headgroup region equal that of bulk water? This assumption is routinely made in determining the number of water molecules per lipid.

The component volumes investigated here may also be useful in "liquid crystallography" methods, such as those that have been developed by Wiener and White (1991a,b, 1992a,b) for structure determination of fluid bilayers. They have used the average transbilayer distribution of molecular fragments to describe the structure of a dioleoylphosphatidylcholine (DOPC) bilayer. Using a combination of x-ray and neutron diffraction data, their technique has given the most complete "image" of a fluid bilayer. These diffraction studies used a joint-refinement procedure that obtains a best fit for the positions (Z_i) and widths (A_i) of submolecular fragments, each represented by a Gaussian distribution along the bilayer normal. The model is fit simultaneously to the x-ray and neutron scattering data to minimize the joint crystallographic R-factor

$$R = \sum_{\substack{j=\text{x-ray,}\\ \text{neutron}}} R_j \quad R_j = \frac{\sum_h \| F_j(h) | - | F_j^*(h) \|}{\sum_h | F_j^*(h) |} \tag{3}$$

where the F_j are the structure factors (* denotes the experimental values) and h is the diffraction order. As a test of their bilayer structure determination, Wiener and White combined a set of component volumes derived from a review of the literature with their calculated fragment distributions to examine packing along the bilayer normal (figure 7 of Wiener and White, 1992b). In Fig. 2 (*solid line*), we use their data to plot the ratio of calculated slab volume (from their fragment distributions and component volumes) to the actual slab volume (from the molecular surface area and slab thickness). Ideally this quantity would equal 1 at all positions along the normal; however, the root mean square deviation from unity is ~7%. Two possibilities for this discrepancy are inaccuracies in either fragment volumes or fragment distributions. To answer the question of fragment volume accuracy, we will calculate these same quantities from simulation and compare our results to the previously published values. To address the latter possibility, we will include a third term in the joint refinement technique of Wiener and White that restrains the slab volume along the bilayer normal to its correct value.

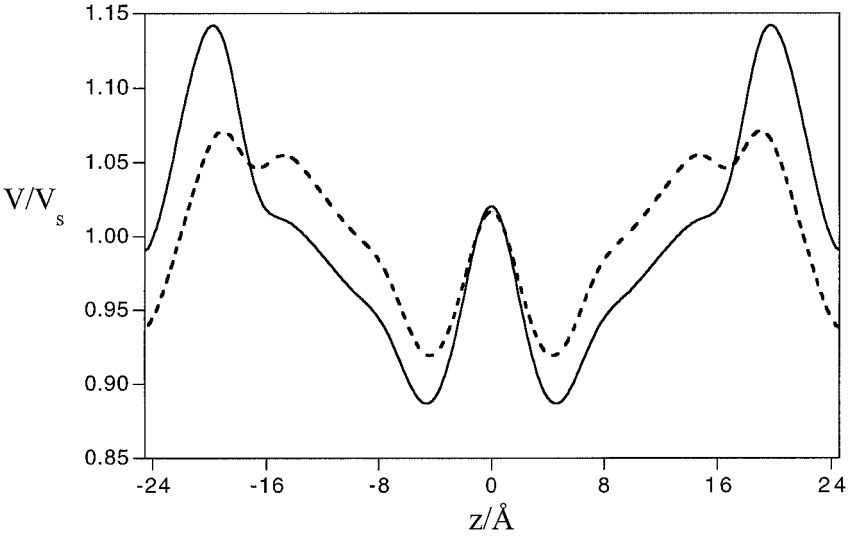

FIGURE 2 Ratio of calculated volume, $(\Sigma_i n_i V_i)/V_s$, using the number densities of Wiener and White (1992b), with their fragment volume data (——) and the values reported here (– – –).

The inclusion of volumetric constraints in the joint-refinement procedure could improve the accuracy of the Wiener and White DOPC structure determination, and it may allow refinement of more fully hydrated membrane systems. The number of structural parameters (Z_i and A_i) determined in the joint refinement is limited by the number of observed diffraction orders. At low hydration (5.36 waters/lipid), Wiener and White were able to observe eight orders from both x-ray and neutron diffraction. At full hydration it is difficult to obtain more than approximately four orders because of thermal fluctuations (Nagle et al., 1996), making the method inapplicable to the study of the fully hydrated systems considered more representative of biological membranes. The addition of volumetric information can increase the number of "experimental" data points, allowing solutions where fewer diffraction orders are observed.

In the next section, the procedures used to extract fragment volumes and to incorporate them into the joint refinement procedure are outlined. In the Results section we calculate component volumes for saturated and unsaturated phosphatidylcholines at various hydration levels. Estimates of the precision of these values and their dependence on bilayer position and lipid composition are also reported. We then demonstrate an application of these data by including volumetric constraints in the bilayer structure determination method developed by Wiener and White.

PROCEDURE

Volumes of submolecular fragments

The procedure for extracting fragment volumes from molecular dynamics (MD) simulations has been described previously (Petrache et al., 1997). Here we give a brief outline of the method. First, the lipid molecule is partitioned into a number of fragments (see Fig. 1 for the scheme used to describe dipalmitoylphosphatidylcholine (DPPC)). The time-averaged transbilayer distribution of submolecular groups is then obtained from the MD simulation trajectory by determining the electron density due to each group in a large number (500 in this case) of slabs (see Fig. 3). The contributions from each of the *i* groups are then converted to a number density $n_i(z)$ after division by the number of electrons in each group. Each cross-sectional slab of area A with thickness Δz will have a volume, V_s, equal to $A \times \Delta z$. Each slab must obey the following relation:

$$V_s = \sum_{i=1}^{\#\text{ of components}} n_i(z) \times V_i \quad (4)$$

As the simulation is divided into a number of equally sized slabs, the optimal set of V_i can be found by minimizing

$$F = \sum_{j=1}^{\#\text{ of slabs}} \left(V_s - \sum_{i=1}^{\#\text{ of components}} n_i(z_j) \times V_i \right)^2 \quad (5)$$

The minimization of F as a function of the component volumes, V_i, was carried out with the program Excel (Microsoft Corporation, version 6.0) using a Newton-Raphson algorithm.

Previously published simulations of DPPC (Feller et al., 1997a) and DOPC (Feller et al., 1997b) were analyzed for this study, as were a simulation of palmitoyloleoyl phosphatidylcholine (POPC) and a second DPPC simulation (denoted DPPC-2) that differed in its hydration level. The investigation of unsaturation effects is chosen to give volume data to experimentalists for the study of this biologically relevant class of lipid, and because unsaturation increases disorder and fluidity in membranes, and thus important differences in the packing of the hydrocarbon chains may be observed in these comparisons. Each simulation system contained 72 lipids with 29.5, 5.36, 13.5, and 15.0 waters/lipid for the DPPC-1, DOPC, POPC, and DPPC-2 simulations, respectively. The simulations ranged in length from 0.5 to 1.5 ns. The simulation protocol was as

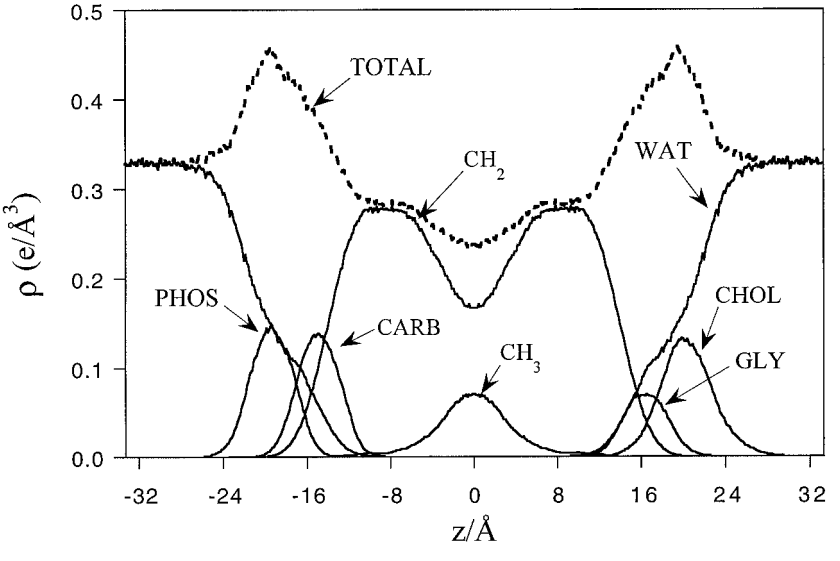

FIGURE 3 Electron density profile for DPPC (– – –) and the contributions from the components defined in Fig. 1 (——). The electron density for each group is divided by the number of electrons per group to obtain number density distributions. For clarity, the headgroup distributions from only one-half of each bilayer are shown.

described previously (Feller et al., 1997a). The program CHARMM (Brooks et al., 1983) was used with the PARM22 all-atom parameter set (Schlenkrich et al., 1996; Feller et al., 1997b). Three-dimensional periodic boundary conditions were employed, and all electrostatic interactions were included via the Ewald sum (Essman et al., 1995). A constant pressure of 1 atm was maintained by allowing the cell length along the bilayer normal to fluctuate. A time step of 2.0 fs was employed along with the SHAKE (Ryckaert et al., 1977) algorithm to constrain bond lengths involving hydrogen atoms. Coordinates were saved at 1-ps intervals for subsequent analysis.

Application to joint-refinement procedure

The volumetric information extracted from simulation was used to augment the joint-refinement method of Wiener and White (1991a,b, 1992a,b) by including a third term,

$$R_{\text{volume}} = \left\langle \left(\frac{V_s - \sum_i n_i V_i}{V_s} \right)^2 \right\rangle^{1/2} \quad (6)$$

where V_s is the slab volume, V_i is the fragment volume, the n_i are determined from the Gaussian distributions being refined, and the brackets denote an averaging over all slabs. This term serves as a packing restraint in the structure determination when combined with the diffraction *R* factors (although Eq. 6 is not of the same form as the diffraction *R* factors, we will adopt the *R* factor terminology for this restraint). Using the x-ray and neutron structure factors for DOPC (Wiener and White, 1992b) and the fragment volumes extracted from simulation, the structure of DOPC was determined by minimizing

$$R = R_{\text{x-ray}} + R_{\text{neutron}} + R_{\text{volume}} \quad (7)$$

in terms of the positions and widths of the Gaussian distributions representing the location of each fragment. The optimization procedure was as described for the minimization of Eq. 5. The volumetric *R* factor was calculated as the average over 100 slabs along the *z* axis. A variety of initial conditions were explored, including those used by Wiener and White (1992b) and a set obtained by fitting the Gaussian distributions to the results of the DOPC MD simulation (Fig. 4 *a*). As is discussed further in the next section, results were relatively insensitive to the choice of the initial conditions, with the possible exception of the location of the glycerol fragment. The results presented here employed the initial conditions derived from simulation. For each refinement strategy, either 20 or 50 hypothetical data sets were

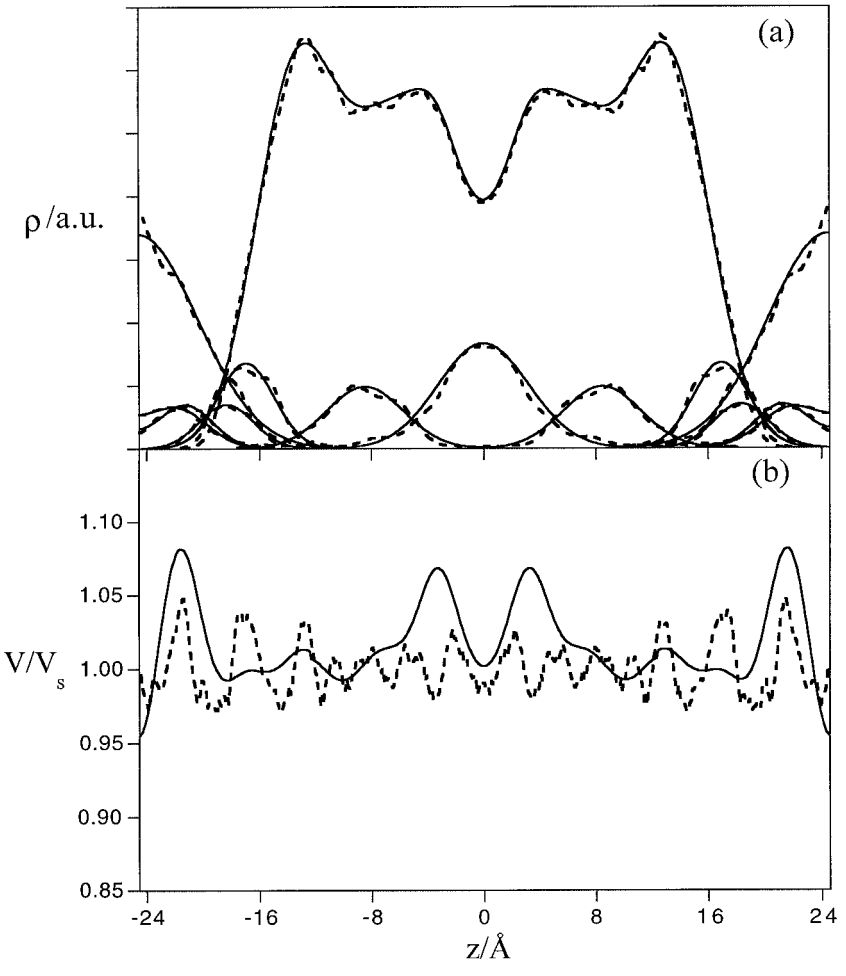

FIGURE 4 (*a*) Best fit of the Gaussian model of Wiener and White (——) to a MD simulation (– – –) of the same system (Feller et al., 1997b). (*b*) The ratio of calculated to actual slab volumes, $(\Sigma_i n_i V_i)/V_s$, using the symmetrized simulation number densities (——) and the best fit of the simulation densities to Gaussians (– – –).

generated from the diffraction structure factors and fragment volumes and their associated standard deviations, using the methods described by Press et al. (1992). The results presented here are based on the fits that converged to lower R values than each of the "self-R" values that measure the uncertainty in the experimental data. These values are given by Wiener and White for the diffraction data (Wiener and White, 1992b), and for the volume data the choice is described in the next section. As noted in Wiener and White's original joint-refinement work, some fits converged to results that passed all of the R tests but placed the glycerol fragment near $d/2$ (where d is the length of the unit cell). Following Wiener and White, unphysical structures with $Z_{GLY} - Z_{CARB} > 5.0$ Å were discarded.

RESULTS

Volumes of submolecular fragments

Each of the four simulations analyzed was broken into 100-ps blocks, the time-averaged density profiles were obtained for each segment, and the optimal fragment volumes were determined from minimization of Eq. 5. Table 1 lists the average component volumes for each simulation, along with the standard error calculated from the fluctuation among subaverages. The results for fully hydrated DPPC (DPPC-1) are in excellent agreement with the preliminary results presented for this system (Petrache et al., 1997), which were based on a somewhat shorter trajectory. For many components, changes in volume due to hydration level or chain unsaturation are undetectable with the present simulations. To determine statistically significant differences between simulations, we applied Student's t-test to the data and determined p values for pairs of component volumes. Using $p < 0.01$ as the criteria, we found no statistically significant differences between the two saturated lipid simulations (DPPC-1 and DPPC-2) or between the unsaturated lipid simulations (POPC and DOPC). Statistically significant differences, however, were found between some saturated and unsaturated lipids for methyl and water fragments. These can be attributed to the ~25°C temperature difference between the simulations, and simulations of bulk water and bulk hexadecane were carried out over this temperature range, which confirmed the observed temperature dependence. Additional statistically significant differences were found between the saturated and unsaturated lipids for headgroup volumes, but this discrepancy may be an artifact of the fitting procedure caused by some groups lying mostly parallel to the plane of the membrane. If the density of the two groups is located largely in the same region along z, the volume of the slab can be assigned to either group and give essentially the same quality fit. The combined volume for both phosphate and choline, and for glycerol and carbonyl, was computed from each simulation, and in these quantities no statistically significant differences were observed among simulations. The individual headgroup fragment volumes, however, are the least well resolved in the present analysis.

The principal assumption within this calculation of component volumes is that the volumes are independent of location within the membrane, e.g., the volume of methylenes near the headgroup is equal to the volume near the bilayer center. Support for this assumption comes from examining the difference between the total volume in each slab and the value calculated from the best fit results. In Fig. 5 we display this quantity for DOPC, using the results in Table 1 with the time-averaged number densities, showing root mean square (rms) deviations of 2.7%, uniformly distributed along the bilayer normal. As a second test, we calculated this error function for the set of 10 trajectory blocks and then averaged the error function over the 10 samples, and the results were nearly identical to the Fig. 5 results, with the rms errors again measuring 2.7%. We also carried out volume fits that included only certain regions of the simulation cell, but were unable to find statistically significant changes in water or methylene volume as a function of position along the membrane.

A primary goal of this work is to provide a set of component volumes for a variety of model-building and experimental applications. We have combined the results of the DPPC-1, POPC, and DOPC simulations (using the computed standard deviations as weights) to obtain a set of average phospholipid component volumes (Table 2). Al-

TABLE 1 Lipid component volumes extracted from MD simulations

Component	DPPC-1	DPPC-2	POPC	DOPC
CH_3	53.62 ± 0.34	53.51 ± 0.91	50.41 ± 0.77	52.79 ± 0.40
CH_2	27.99 ± 0.06	27.87 ± 0.10	28.24 ± 0.17	28.13 ± 0.09
C=C	N/A	N/A	42.14 ± 2.31	45.91 ± 0.69
CARB	44.09 ± 1.05	43.07 ± 0.64	38.43 ± 1.47	37.40 ± 1.28
GLY	63.59 ± 2.11	67.35 ± 1.28	72.48 ± 2.28	81.62 ± 2.96
PHOS	65.63 ± 2.95	67.08 ± 2.08	52.12 ± 2.23	51.05 ± 6.31
CHOL	108.60 ± 2.49	105.92 ± 1.98	120.68 ± 2.98	129.68 ± 5.25
WAT	30.42 ± 0.04	30.38 ± 0.07	29.52 ± 0.10	*
CARB+GLY	151.77 ± 0.54	153.49 ± 0.42	149.34 ± 1.01	156.42 ± 8.71
PHOS+CHOL	174.23 ± 0.62	173.00 ± 0.37	172.80 ± 0.98	180.72 ± 5.78

Values are in Å^3. Error estimates are one standard error, $\sigma/\sqrt{N}$. DPPC-1 and DPPC-2 refer to simulations with 29 and 15 waters/lipid, respectively.
*The volume per water molecule was fixed at 29.5 Å^3.

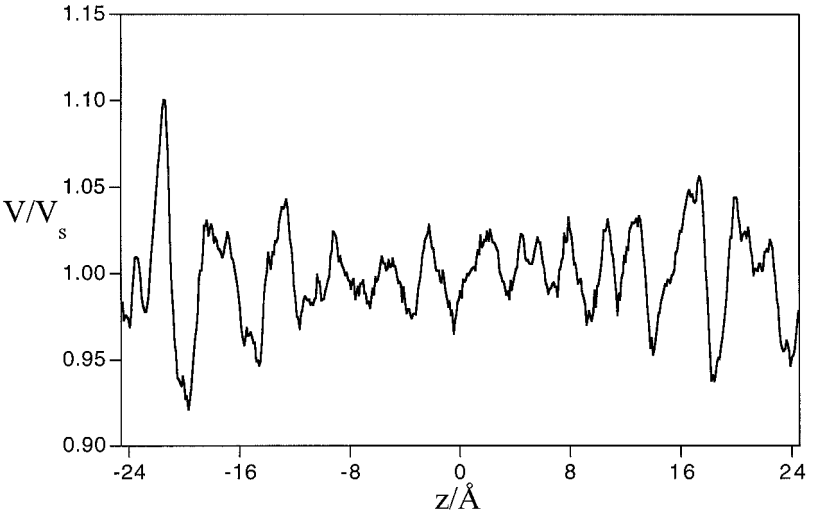

FIGURE 5 The ratio of calculated to actual slab volumes, $(\Sigma_i n_i V_i)/V_s$, from the best-fit volumes and the time-averaged simulation distributions, as a function of position within the membrane.

though some statistically significant differences were observed between simulations (most notably, the thermal expansion of alkane and water), these are likely comparable to changes that would be observed from a new set of simulations using an alternative potential energy parameter set. Therefore, we have chosen to pool all of our data to form a single set of volumes. To assess the validity of these component volumes, we calculated the molecular volumes of DPPC, POPC, and DOPC to obtain 1212, 1257, and 1302 $Å^3$, in very good agreement with the experimental values of 1232, 1267, and 1295 $Å^3$, respectively (Nagle and Wiener, 1988; Small, 1986; Wiener and White, 1992a). The calculated headgroup volume, which included the carbonyl, glycerol, phosphate, and choline fragments, is 321 $Å^3$, compared to experimental values of 319 and 325 $Å^3$ (Sun et al., 1994; Small, 1967).

Application to joint-refinement procedure

Having obtained a set of component volumes that appear to be transferable among lipids and that agree with available experimental data on molecular and headgroup volumes, it is now possible to include these data in the diffraction refinement procedure used by Wiener and White in their studies of DOPC bilayers. We begin by combining our fragment volumes with the number distributions obtained by Wiener and White (1992b), using solely their diffraction data. The results are displayed in Fig. 2 (*dashed line*) and are an improvement over the solid line in the same figure, which was derived from the fragment volumes cited by Wiener and White (rms deviation of ~5% versus ~7%). If we assume that all of the remaining deviation is due to errors in the number densities, there are at least two sources of error to consider. First, there could be inaccuracies in the measured diffraction orders. Second, the fitting procedure may introduce errors by imposing a Gaussian distribution on each fragment density. We can investigate this second source of error by examining our MD simulation of DOPC. In Fig. 4 *a*, the number densities obtained from the DOPC simulation were fit to the Gaussian form used to describe the location of each fragment (the methylenes are represented by a sum of three Gaussians, with each function representing N methylene groups). In Fig. 4 *b*, we have the ratios of calculated to actual slab volume, with solid lines representing the raw simulation results and dashed lines corresponding to the best fit of the simulation densities to Gaussians. From this figure, it is seen that requiring the Gaussian functional form for the fragment distributions leads to deviations in V (rms 3.3% versus 1.8%). Assuming that the simulation distributions are accurate, this gives an approximate lower limit on R_{volume} for any model distribution based on Gaussians. The most pronounced deviations occur in the methyl group region. Previous analysis of this simulation had suggested that the methyl distribution is not well modeled by a Gaussian (Feller et al., 1997b), in accord with the present observations.

To include the volumetric R factor in the refinement procedure, we first determined its expected magnitude from the DOPC simulation data. The results of the best-fit simulation densities to Gaussians (e.g., the Z_i and A_i) shown in Fig. 4 *a* are reported in Table 3. The value of R_{volume} (Eq. 6), using the data presented graphically in Fig. 4 *a*, was 0.033. We take this as a measure of the "experimental noise" in our volume constraint calculation. As this value is the same magnitude as the x-ray and neutron self-R values,

TABLE 2 Average lipid component volumes extracted from all MD simulations (weighted by the standard deviations among subaverages)

Group	Volume/$Å^3$
CH_3	52.7 ± 1.2
CH_2	28.1 ± 0.1
C=C	45.0 ± 1.6
CARB	39.0 ± 1.4
GLY	68.8 ± 9.9
PHOS	53.7 ± 2.4
CHOL	120.4 ± 5.0

The error estimates are the standard deviations among the lipids.

TABLE 3 Parameters for the best fit of the Gaussian model of Weiner and White (1992) to a MD simulation of the same system (Feller et al., 1997b), that were subsequently used as initial conditions for the joint-refinement procedure

Group	*Z*	*A*	*N*
CH_3	0.0	4.57	
$CH_2(1)$	3.26	2.04	0.75
$CH_2(2)$	5.98	5.95	16.44
$CH_2(3)$	13.57	3.95	10.81
C=C	8.47	3.89	
CARB	16.94	2.81	
GLY	18.34	2.73	
PHOS	21.28	2.75	
CHOL	21.85	3.02	
WAT	24.55	6.00	

The results are displayed graphically in Fig. 4.

the volumetric *R* factor was given the same weight as the diffraction *R* values when we carried out the minimizations. In the joint refinements to be discussed next, the criterion for a successful fit to the volume data was $R_{volume} < 0.065$, so that the fit to the volume data had to be equal to that for the neutron and better than that for the x-ray.

In their joint refinement of the structure of DOPC, Wiener and White kept the distribution of CH_3, C=C, and H_2O groups fixed at values they determined independently in separate experiments. The positions and widths of the Gaussians representing carbonyl, glycerol, phosphate, and choline groups were free parameters, as were the number (N_i), position, and width of the three distributions representing the methylene groups, for a total of 17 parameters. Using the relation that the sum of the methylene N_i must be 28, the number of parameters is reduced to 16. Combining their diffraction data with the present volumetric constraints, we repeated the refinement procedure; the parameter values obtained are presented in Table 4, along with a set of their original results for comparison. The results from the two different procedures are in excellent agreement. Although the present method includes additional restraints, a better fit to the x-ray and neutron data was obtained than in the original work. Furthermore, the fraction of refinements that were successful increased upon addition of the volume restraint.

The number of structural parameters that can be determined in the refinement is fixed by the number of available data points. In addition to minimizing the difference between the 16 calculated and measured structure factors, eight additional pieces of data have been included via the fragment volumes used to calculate R_{volume}. These additional data allow more complex models of the lipid bilayer to be investigated, e.g., by allowing fragments with positions fixed in the analysis of Wiener and White to vary as additional parameters. Beginning with the membrane interior, the position and width of both the methyl and C=C groups were included in the refinement procedure, and the resulting 20-parameter model was fit to the combined diffraction and volumetric data. The results, presented in Table 4, suggest that allowing the location of the methyl density to vary has no benefit, as every refinement trial ended with both methyl Gaussians (representing the individual monolayers) at the same position in the center of the membrane. Subsequent refinements were thus carried out with the methyl density fixed at zero. The values obtained via refinement for the methyl and C=C widths are in good agreement with those assumed by Wiener and White, and the C=C position is found to be 0.34 Å closer to the headgroup in the present analysis. The double bond, with its reduced number of hydrogens, scatters neutrons more strongly than methylene segments, and the experimentally determined neutron scattering density has a small peak at ~8.3 Å, consistent with the present determination of $Z_{C=C} = 8.22$ Å. The difficulty in determining global minima in the refinement is highlighted by comparison of the 16- and 20-parameter model results. Increased values of $R_{x\text{-}ray}$ and R_{total} were obtained with the 20-parameter model, presumably

TABLE 4 A comparison of the joint refinement results obtained with and without (from Wiener and White, 1992b) volumetric constraints

	16-parameter model			20-parameter model			Wiener and White (1992b)		
Group	*Z*	*A*	*N*	*Z*	*A*	*N*	*Z*	*A*	*N*
CH_3	0.00 ± 0.00*	2.95 ± 0.28*		0.00 ± 0.00	3.00 ± 0.17		0.00 ± 0.00*	2.95 ± 0.28*	
$CH_2(1)$	3.70 ± 0.16	1.61 ± 0.13	1.04 ± 0.16	3.72 ± 0.11	1.62 ± 0.22	0.97 ± 0.18	2.95 ± 0.77	2.84 ± 0.63	3.67 ± 2.64
$CH_2(2)$	6.29 ± 0.27	5.44 ± 0.29	13.49 ± 0.81	6.28 ± 0.31	5.33 ± 0.21	13.86 ± 1.40	6.09 ± 1.43	3.88 ± 1.04	7.18 ± 2.58
$CH_2(3)$	13.57 ± 0.15	4.71 ± 0.12	13.47 ± 0.79	13.61 ± 0.25	4.61 ± 0.18	13.20 ± 1.28	12.76 ± 0.59	5.19 ± 0.45	17.15 ± 2.51
C=C	7.88 ± 0.09*	4.29 ± 0.16*		8.22 ± 0.61	4.52 ± 0.51		7.88 ± 0.09*	4.29 ± 0.16*	
CARB	15.94 ± 0.06	2.72 ± 0.06		16.00 ± 0.07	2.71 ± 0.08		15.99 ± 0.06	2.77 ± 0.12	
GLY	18.82 ± 0.17	2.27 ± 0.12		18.82 ± 0.22	2.25 ± 0.19		18.67 ± 0.42	2.46 ± 0.38	
PHOS	20.13 ± 0.08	3.09 ± 0.08		20.16 ± 0.10	3.04 ± 0.10		20.15 ± 0.13	3.09 ± 0.16	
CHOL	21.98 ± 0.11	3.45 ± 0.20		21.96 ± 0.16	3.55 ± 0.41		21.86 ± 0.22	3.48 ± 0.52	
$R_{x\text{-}ray}$	0.012			0.025			0.022		
$R_{neutron}$	0.051			0.048			0.062		
R_{volume}	0.047			0.047			N/A		

Error estimates are the standard deviation among successful refinements.

*Values that were not included in the joint-refinement procedure, but were fixed at values obtained from separate experiments.

because of poor initial conditions for the double bond and methyl fragments.

The existence of the volume data also allows refinements of the original 16-parameter model of Wiener and White by combining the volumetric data with the x-ray and neutron data sets individually. The results utilizing neutron data are given on the left side of Table 5, and are in excellent agreement with the combined diffraction results (Table 4). Among the headgroup fragments, the largest discrepancy is in the position of the glycerol (0.34 Å), with the remaining pieces within ~0.1 Å of the combined data results. Refinements utilizing only x-ray and volume data, however, were unable to resolve the location of the glycerol and carbonyl fragments, with more than half of the structures having $Z_{CARB} > Z_{GLY}$. After discarding these unphysical results, the remaining successful refinements were averaged; the results given on the right side of Table 5. Although the carbonyl and glycerol fragments differ significantly from the Table 4 results, agreement is quite good for the phosphatidylcholine structure. An interesting observation from these calculations is that the neutron data seem much more compatible with the volumetric information than the x-ray data, with the neutron + volume calculation obtaining an R_{volume} value that is less than one-fifth that of the x-ray + volume refinement.

The additional degrees of freedom available in the refinement can also be used to increase the number of Gaussian functions representing the methylene density. Fitting the methylene density from the MD simulation (Feller et al., 1997b) to a set of four Gaussians significantly improved the agreement (the improvement on going from three to four functions was as great as that upon changing from two to three). The additional Gaussian requires three more parameters, for a total of 22 degrees of freedom (the methyl density was assumed to be fixed at zero, as discussed in the previous paragraph). This model was refined, but no significant reduction in R was observed over the three-Gaussian model. We did observe that the methylene density distribution obtained with four Gaussians is narrower, i.e., there is less overlap of the hydrocarbon and headgroup regions. The largest effect on the headgroup is seen in the glycerol fragment, which moves 0.22 Å to the interior, with its $1/e$ half-width increasing by 0.28 Å. As it appears that the addition of a fourth Gaussian to describe the methylene region offers little or no advantage with the present data set, we employed the three-Gaussian model proposed by Wiener and White for all subsequent analysis. It should be noted that in testing various representations for the methylene density, models using only two Gaussians obtained nearly the same levels of R as the three- and four-Gaussian representations. This suggests that it may be possible to determine the structure of membranes for which fewer experimental data are available, by simplifying the methylene representation.

The water density was represented by two Gaussian distributions fixed at $Z = \pm 22.51$ Å in the joint refinement of Wiener and White (1992a,b), although they noted that it could be equally well described by a single function located at $d/2$, i.e., $Z = 24.55$ Å (Wiener et al., 1991). By allowing both the position and half-width of the water distribution to be free parameters, a total of 21 parameters were fit to the 24 pieces of diffraction and volume data. Two sets of initial conditions were investigated that differed only in the starting positions and half-widths of the water distribution. The first used the values of Wiener and White, and the second set came from the fit of Gaussian distributions to the MD simulation data (although the simulation data fit a single function best, the refinement carried out with these initial conditions allowed for a pair of distribution functions). The results are given in Table 6. Whereas both water distributions stayed near their respective initial conditions, the remaining fragment distributions moved from the initial conditions and under both protocols converged to similar final results. As the R_{total} obtained with a single water function centered at $d/2$ was lower than that obtained from the Wiener and White initial conditions, and because the single distribution requires the determination of one less parameter, we adopt a single Gaussian representation for our final model.

TABLE 5 A comparison of the refinement results obtained by combining volumetric constraints with neutron (left) and x-ray (right) data sets

	Neutron			X-ray		
Group	Z	A	N	Z	A	N
$CH_2(1)$	3.08 ± 0.15	2.03 ± 0.11	1.16 ± 0.23	3.94 ± 0.12	3.46 ± 0.12	7.02 ± 0.62
$CH_2(2)$	5.06 ± 0.37	4.10 ± 0.32	10.07 ± 1.95	9.21 ± 0.38	4.83 ± 0.24	10.46 ± 0.59
$CH_2(3)$	12.36 ± 0.32	5.24 ± 0.43	16.77 ± 1.81	14.33 ± 0.19	4.60 ± 0.22	10.52 ± 0.53
CARB	15.99 ± 0.04	2.77 ± 0.07		16.29 ± 0.19	3.22 ± 0.17	
GLY	18.44 ± 0.13	2.58 ± 0.21		18.43 ± 0.74	3.44 ± 0.34	
PHOS	20.24 ± 0.11	3.13 ± 0.09		19.82 ± 0.38	3.24 ± 0.16	
CHOL	22.09 ± 0.08	3.64 ± 0.18		21.84 ± 0.17	3.25 ± 0.29	
$R_{x\text{-}ray}$		0.262			0.050	
$R_{neutron}$		0.039			0.168	
R_{volume}		0.009			0.047	

Error estimates are the standard deviation among successful refinements.

TABLE 6 A comparison of structures obtained with different initial positions of the water distribution

Group	Z	A	N	Z	A	N
CH_3	0.00	3.01 ± 0.15		0.00	3.00 ± 0.18	
$CH_2(1)$	3.70 ± 0.18	1.63 ± 0.17	0.98 ± 0.18	3.69 ± 0.20	1.63 ± 0.16	0.99 ± 0.17
$CH_2(2)$	6.44 ± 0.30	5.49 ± 0.29	14.43 ± 1.13	6.38 ± 0.37	5.44 ± 0.39	14.19 ± 1.46
$CH_2(3)$	13.70 ± 0.21	4.58 ± 0.18	12.59 ± 1.07	13.66 ± 0.26	4.63 ± 0.23	12.82 ± 1.37
C=C	8.36 ± 0.69	4.53 ± 0.69		8.35 ± 0.59	4.55 ± 0.45	
CARB	15.99 ± 0.07	2.72 ± 0.08		15.99 ± 0.09	2.68 ± 0.13	
GLY	18.85 ± 0.29	2.29 ± 0.18		18.89 ± 0.25	2.27 ± 0.20	
PHOS	20.18 ± 0.11	3.08 ± 0.09		20.16 ± 0.10	3.08 ± 0.10	
CHOL	21.78 ± 0.45	3.53 ± 0.31		21.88 ± 0.25	3.53 ± 0.30	
WAT	22.81 ± 0.69	4.56 ± 0.30		24.55 ± 0.00	5.49 ± 0.45	
$R_{\text{x-ray}}$		0.049			0.013	
R_{neutron}		0.050			0.042	
R_{volume}		0.045			0.046	

Error estimates are the standard deviation among successful refinements.

After examining a number of models to describe the transbilayer distribution of molecular fragments, we choose a 20-parameter model that assumes the methyl density to be centered around $z = 0$, the water density to be centered around $d/2$, and the methylene density to be represented by the sum of three Gaussian distributions. The resulting structure is shown graphically in Fig. 6 (parameter values are listed in Table 6), along with the original results of Wiener and White. The agreement between the refinement results with and without volumetric restraints is excellent. The agreement with the x-ray and neutron diffraction results is as good or better with volumetric data, even though this technique imposes additional constraints on the fitting procedure (some of the improvement, however, may be from

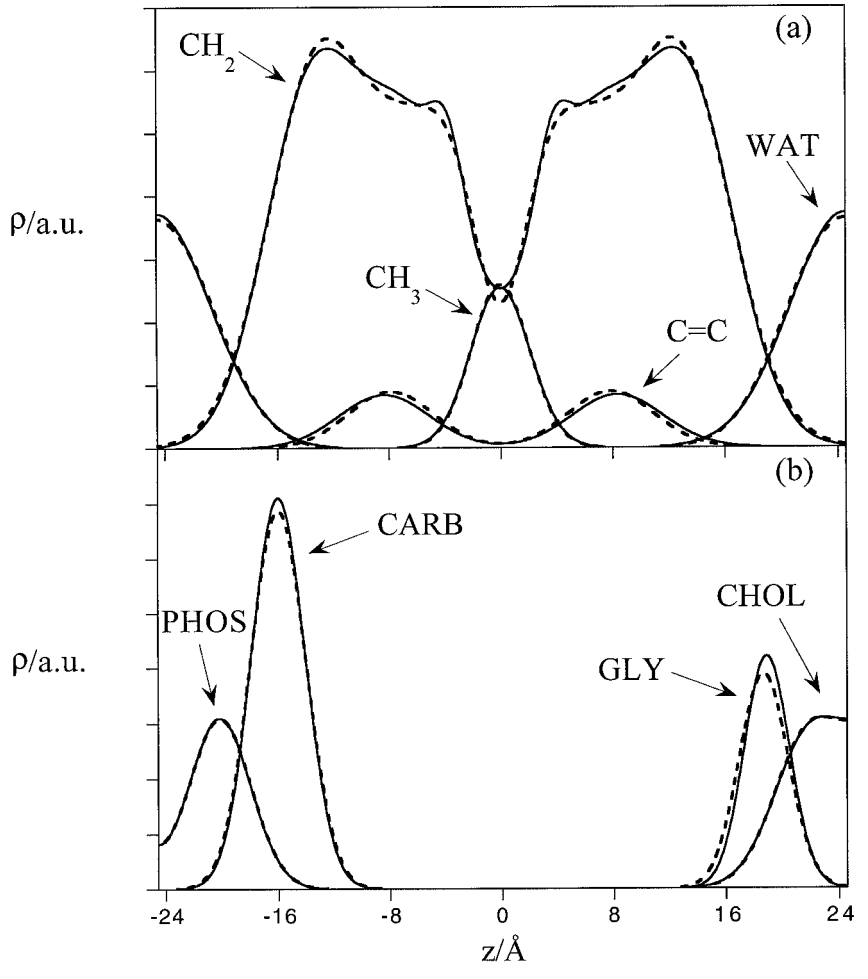

FIGURE 6 Structure of DOPC. The dashed lines show the results of Wiener and White (no volumetric restraints), and the solid lines display the results listed in Table 6 (right hand side).

the increased flexibility allowed by a 20-parameter model). A notable result from the present refinement is that 84% of the refinements were successful (the remainder did not meet the $R_{neutron}$ criteria), compared with a ~10% success rate reported by Wiener and White and the ~50% we observed in our first trials (e.g., Table 4 results). The most significant difference between the structures depicted in Fig. 6 is the location of the double bond, but this discrepancy is still less than 1 Å and, as mentioned previously, is supported by the small peak in the neutron scattering profile at ~8.3 Å.

For our final result, we investigate the possibility of weighting the R_{volume} factor differently from the diffraction R factors in the refinement procedure. As a test, we undertook refinements with $R_{total} = R_{neutron} + R_{x\text{-}ray} + 5 \times R_{volume}$, and the resulting structure for this calculation is given in Table 7. The values of R_{volume} decreased by nearly 50%, and although the diffraction R values increased, over half the refinements were successful (i.e., diffraction R values less than the self-R). The most significant changes in the structure were the width of the methyl distribution, which increased by ~8%, and the location of the glycerol and choline groups, which both moved toward the interior of the membrane. Additional calculations using a four-Gaussian model of the methylene region showed the same trends, with the glycerol group moving an additional 0.5 Å to the interior. These calculations show the power of combining x-ray, neutron, and volumetric data. In the phospholipid headgroup, for example, the phosphate and carbonyl groups can be determined unambiguously from the x-ray and neutron diffraction experiments, respectively. The refinement procedure can place the glycerol and choline fragments, which do not lead to peaks in either scattering profile, based largely on packing considerations. Although in the present work we have used two possible relative weights for the volume data, this should ultimately be determined by an analysis of the estimated relative error in the three data sets.

TABLE 7 Refinement results for $R_{total} = R_{neutron} + R_{x\text{-}ray} + 5 \times R_{volume}$

Group	Z	A	N
CH_3	0.0	3.25 ± 0.20	
CH_2(1)	3.62 ± 0.48	2.32 ± 0.26	1.03 ± 0.33
CH_2(2)	5.53 ± 0.52	4.94 ± 0.48	12.08 ± 2.10
CH_2(3)	12.98 ± 0.46	4.96 ± 0.41	14.89 ± 1.93
C=C	8.38 ± 0.76	4.40 ± 0.42	
CARB	16.02 ± 0.10	2.75 ± 0.13	
GLY	18.64 ± 0.41	2.71 ± 0.33	
PHOS	20.17 ± 0.10	3.05 ± 0.13	
CHOL	21.21 ± 0.52	3.74 ± 0.69	
WAT	24.55	4.74 ± 0.58	
$R_{x\text{-}ray}$		0.045	
$R_{neutron}$		0.075	
R_{volume}		0.025	

Error estimates give the standard deviation among successful refinements.

DISCUSSION

As this work has demonstrated, the synthesis of information obtained from laboratory experiments and computational studies has tremendous potential in the study of bilayer membranes. From atomic-level molecular dynamics simulations, the volumes of submolecular lipid fragments were obtained directly, where in the past, volume estimates at this level of detail came indirectly from the interpretation of experimental data. Although most component volumes were not obtained at the level of precision at which the molecular volume is measured experimentally (<0.5%), longer simulations offer the opportunity to reduce the error bars associated with these results. This would be especially valuable for the headgroup components that are least well resolved in the present study. Comparison of the molecular volume and headgroup volumes calculated from the simulation results with experiment show differences of <1%, however, lending support to the validity of the volumes derived here.

The volumetric data obtained from simulation were shown to be useful in the liquid-crystallography refinement of bilayer structure from diffraction data. As described by Wiener and White (1991a,b), a primary limit on the complexity of the model describing the membrane is the requirement that the number of parameters, or degrees of freedom, in the model must not exceed the number of experimental data points. To reduce the degrees of freedom, separate experiments were carried out to determine the distribution of the CH_3, C=C, and water fragments before the joint refinement. The need to reduce the degrees of freedom thus necessitated additional experiments, including specific deuteration of the double bond. We have demonstrated the feasibility of a second approach, the inclusion of additional "experimental" data points representing the volume of each submolecular fragment. Via this method, the structure of DOPC was solved solely on the basis of the primary diffraction experiments and the simulation-based volumes, i.e., without relying on extra information from specific labeling studies. Furthermore, the degrees of freedom afforded by the inclusion of volumetric data allowed a more complex representation of the methylene region and allowed us to investigate one versus two Gaussian representations of the terminal methyl and water distributions.

We thank the Stanley Rall research program at Whitman College for financial support. This work was supported in part by the Phillips Laboratory, Air Force Material Command, United States Air Force, through the use of the IBM SP2 at the Maui High Performance Computing Center, and by the National Science Foundation through grant MCB-9728206.

REFERENCES

Brooks, B. R., R. E. Bruccoleri, B. D. Olafson, D. J. States, S. Swaminathan, and M. Karplus. 1983. CHARMM: a program for macromolecular energy, minimization, and dynamics calculations. *J. Comp. Chem.* 4:187–217.

Essman, U., L. Perera, M. L. Berkowitz, T. Darden, H. Lee, and L. G. Pedersen. 1995. A smooth particle mesh Ewald method. *J. Chem. Phys.* 103:8577–8593.

Feller, S. E., R. M. Venable, and R. W. Pastor. 1997a. Computer simulation of a DPPC phospholipid bilayer: structural changes as a function of molecular surface area. *Langmuir.* 13:6555–6561.

Feller, S. E., D. Yin, R. W. Pastor, and A. D. MacKerell. 1997b. Molecular dynamics simulation of unsaturated lipid bilayers at low hydration: parameterization and comparison with diffraction studies. *Biophys. J.* 73:2269–2279.

Hoover, W. G. 1995. Canonical dynamics: equillibrium phase-space distributions. *Phys. Rev. A.* 31:1695–1697.

Koenig, B. W., H. H. Strey, and K. Garwisch. 1997. Membrane lateral compressibility determined by NMR and x-ray diffraction—effect of acyl chain polyunsaturation. *Biophys. J.* 73:1954–1966.

McIntosh, T. J., and S. A. Simon. 1986. Area per molecule and distribution of water in fully hydrated dilauroylphosphatidylethanolamine bilayers. *Biochemistry.* 25:4948–4952.

Nagle, J. F. 1993. Area/lipid of bilayers from NMR. *Biophys. J.* 64: 1476–1481.

Nagle, J. F., and D. A. Wilkinson. 1978. Lecithin bilayers: density measurements and molecular interactions. *Biophys. J.* 23:159–175.

Nagle, J. F., R. Zhang, S. Tristram-Nagle, W. Sun, H. Petrache, and R. M. Suter. 1996. X-ray structure determination of fully hydrated L_α phase dipalmitoylphosphatidylcholine bilayers. *Biophys. J.* 70:1419–1431.

Petrache, H. I., S. E. Feller, and J. F. Nagle. 1997. Determination of component volumes of lipid bilayers from simulation. *Biophys. J.* 72: 2237–2242.

Press, W. H., S. A. Teukolsky, W. T. Vettering, and B. P. Flannery. 1992. Numerical Recipes. Cambridge University Press, New York.

Ryckaert, J. P., C. Cicotti, and H. J. C. Berendsen. 1977. Numerical integration of the cartesian equations of motion of a system with constraints: molecular dynamics of n-alkanes. *J. Comp. Chem.* 23:327–341.

Schlenkrich, M., J. Brickman, A. D. MacKerell, and M. Karplus. 1996. Empirical potential energy function for phospholipids: criteria for parameter optimization and applications. *In* Biological Membranes: A Molecular Perspective from Computation and Experiment. K. Merz, and B. Roux, editors. Birkhäuser, Boston. 31–81.

Seelig, A., and J. Seelig. 1974. Dynamic structure of fatty acyl chains in a phospholipid bilayer measured by DMR. *Biochemistry.* 13:4839–4845.

Small, D. M. 1967. Phase equilibria and structure of dry and hydrated egg lecithin. *J. Lipid Res.* 8:551–557.

Small, D. M. 1986. The Physical Chemistry of Lipids, Handbook of Lipid Research, Vol. 4. Plenum Press, New York.

Sun, W. J., R. M. Suter, M. A. Knewtson, C. R. Worthington, S. Tristram-Nagle, R. Zhang, and J. F. Nagle. 1994. Order and disorder in fully hydrated unoriented bilayers of gel phase DPPC. *Phys. Rev. E.* 49: 4665–4676.

White, S. H., R. E. Jacobs, and G. I. King. 1987. Partial specific volumes of lipid and water in mixtures of egg lecithin and water. *Biophys. J.* 52:663–665.

Wiener, M. C., G. I. King, and S. H. White. 1991. Structure of a fluid dioleoylphosphatidylcholine bilayer determined by joint refinement of x-ray and neutron diffraction data. I. Scaling of neutron data and the distributions of double bonds and water. *Biophys. J.* 60:568–576.

Wiener, M. C., S. Tristram-Nagle, D. A. Wilkinson, L. E. Campbell, and J. F. Nagle. 1988. Specific volumes of lipids in fully hydrated bilayer dispersions. *Biochim. Biophys. Acta.* 938:135–142.

Wiener, M. C., and S. H. White. 1991a. Fluid bilayer structure determination by the combined use of x-ray and neutron diffraction. I. Fluid bilayer models and the limits of resolution. *Biophys. J.* 59:162–173.

Wiener, M. C., and S. H. White. 1991b. Fluid bilayer structure determination by the combined use of x-ray and neutron diffraction. II. "Composition-space" refinement method. *Biophys. J.* 59:174–185.

Wiener, M. C., and S. H. White. 1992a. Structure of a fluid dioleoylphosphatidylcholine bilayer determined by joint refinement of x-ray and neutron diffraction data. II. Distribution and packing of terminal methyl groups. *Biophys. J.* 61:428–433.

Wiener, M. C., and S. H. White. 1992b. Structure of a fluid dioleoylphosphatidylcholine bilayer determined by joint refinement of x-ray and neutron diffraction data. III. Complete structure. *Biophys. J.* 61: 434–447.